Received: 13 December 2022 | Revised: 2 May 2023 | Accepted: 3 May 2023

DOI: 10.1002/ese3.1485

ORIGINAL ARTICLE

Deconvolution approach for floating wind turbines

Zirui Liu[1] | Oleg Gaidai[1] | Jiayao Sun[2] | Yihan Xing[3]

[1]College of Engineering Science and Technology, Shanghai Ocean University, Shanghai, China

[2]School of Naval Architecture and Ocean Engineering, Jiangsu University of Science and Technology, Zhenjiang, China

[3]Department of Mechanical and Structural Engineering and Materials Science, University of Stavanger, Stavanger, Norway

Correspondence
Oleg Gaidai, College of Engineering Science and Technology, Shanghai Ocean University, Shanghai, China.
Email: o_gaidai@just.edu.cn

Abstract

Green renewable energy is produced by floating offshore wind turbines (FOWT), a crucial component of the modern offshore wind energy industry. It is a safety concern to accurately evaluate excessive weights while the FOWT operates in adverse weather conditions. Under certain water conditions, dangerous structural bending moments may result in operational concerns. Using commercial FAST software, the study's hydrodynamic ambient wave loads were calculated and converted into FOWT structural loads. This article suggests a Monte Carlo-based engineering technique that, depending on simulations or observations, is computationally effective for predicting extreme statistics of either the load or the response process. The innovative deconvolution technique has been thoroughly explained. The suggested approach effectively uses the entire set of data to produce a clear but accurate estimate for severe response values and fatigue life. In this study, estimated extreme values obtained using a novel deconvolution approach were compared to identical values produced using the modified Weibull technique. It is expected that the enhanced new de-convolution methodology may offer a dependable and correct forecast of severe structural loads based on the overall performance of the advised de-convolution approach due to environmental wave loading.

KEYWORDS

environmental loads, floating offshore wind turbine, green energy, renewable energy, wind energy

1 | INTRODUCTION

A significant amount of the world's energy demands might be met by wind energy, a substantial ecologically benign renewable energy source. Offshore wind farms are commonly constructed to harness plentiful wind energy and produce power. Due to the fact that offshore wind speeds are frequently higher than onshore wind speeds, the floating offshore wind turbine (FOWT)'s contribution to energy generation is essential for the sector.

Predicting FOWT design loads may be done largely in one of the two methods. The recommended design procedure might assist in choosing the ideal wind turbine characteristic values, thereby reducing the risk of structural damage to FOWTs: (a) prediction of severe events and corresponding system responses with a low probability of occurrence, resulting in excessive structural loads and reactions; and (b) extrapolation of system responses and load levels toward cricilevels, while system being simulated/measured under typical operating environmental circumstances.[1–4] Both strategies are advised by the IEC 61400-1 standard.[5–7] The second approach (b), which is elaborated in this research study, promotes techniques that are already shown to be effective for a range of maritime constructions, including various offshore platforms and vessels.[8–13]

There are numerous recently published research studies related to FOWT reliability aspects.[14]

In Zhang et al.[15] authors studied dynamic system fault tree analysis to evaluate quantitatively FOWT failure rates. In Li et al.[16] authors utilized Bayesian Network to analyze FOWT reliability function and reported that the results were in good agreement with the available verified data. In Xu et al.[17] authors have proposed a multidimensional reliability approach to assess site-specific FOWT environmental loads. In Song et al.[18] authors conducted dynamic reliability structural analysis, given FOWT subjected to wind-wave joint excitations, using the so-called probability density evolution method. In Liu et al.[19] authors have used the intelligent teaching-learning-based optimization technique to assess FOWT mooring system reliability functions. In Sultania and Manuel[20] authors have utilized three-dimensional (3D) inverse first-order reliability method to estimate 50-year return period long-term loads acting on FOWT. In Zhang et al.[21] authors used the fuzzy set theory to handle FOWT failure statistics, reported results showed advantages; for example, failure rate reduced errors.

This study uses unique de-convolution to boost the effectiveness of using measured or simulated data. To characterize the tail behavior of the extreme value distribution, the structural load data that are now available are paired with an appropriate class of parametric functions. Then, a comprehensive methodology to estimate extreme values is devised that not only just relies on an asymptotic distribution (peak over threshold) but also is independent of conventional methods like Gumbel, Pareto, Weibull, and POT. With much fewer simulations and observations than the direct MC technique, the recommended MC-based approach for engineering design has the benefit of producing predictions of severe load and response that are comparable to accuracy. Figure 1 left shows the National Data Buoy Center's (NDBC) National Oceanic and Atmospheric Administration (NOAA) database that was used in this study. The Cape Elizabeth location's accessible in situ measured hourly historical metocean data, gathered between 2010 and 2017, have been used to calculate joint wind-wave statistics.[22]

The flow chart for the described long-term MC-based statistical/reliability study is shown in Figure 1 right.

The authors use the term "environmental sea state" to refer to the whole set of locally accounted environmental factors, such as wave height and wind speed, that are included in the in situ environmental sea state, see International Electrotechnical Commission and colleagues[23–33] for current studies on FOWTs and their engineering dependability.

2 | METHOD

Extreme value prediction problems in engineering are frequent and challenging, especially when the available data set is limited.[34–38] Let's take a look at a stationary (ideally ergodic) stochastic of either the load or the response process $X(t)$, which may be described as the sum of two distinct stationary component processes $X_1(t)$ and $X_2(t)$

$$X(t) = X_1(t) + X_2(t). \tag{1}$$

It should be noted that this work promotes a general method that may be used to predict extreme values for a

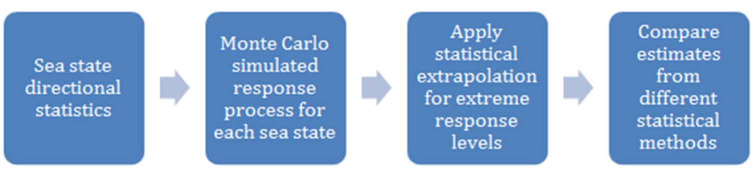

FIGURE 1 Left: Typical data measurement buoy.[11] Right: Flow chart for long-term environmental statistical/reliability analysis.

variety of loads and reactions for different ships and offshore structures. One can derive PDF p_X for the process of interest load/response $X(t)$ in two distinct ways:

A) With the time series $X(t)$ as the available data set, direct de-convolution is used to estimate p_X^A,
B) Separate PDF extraction is performed from the corresponding process components $X_1(t)$ and $X_2(t)$, namely p_{X_1} and p_{X_2} before convolution is applied $p_X^B = \text{conv}(p_{X_1}, p_{X_2})$.

Target PDF p_X estimates both p_X^A and p_X^B . Approach (A) is more straightforward to use; however, (B) would yield a more accurate target PDF p_X. Convolution has the distinct advantage of enabling direct extrapolation of the empirical PDF p_X^A toward target design probability levels without assuming any extrapolation parametric or functional class, such as from the family of generalized extreme value distributions (GEV), which is necessary to extrapolate PDF tail. It should be emphasized that the majority of extrapolation techniques that are often used in offshore engineering practice do, in fact, rely on assuming certain extrapolation parametric/functional classes.[8–33,39–41] Among the widely used techniques, the techniques currently in use are peak over the threshold (POT),[31] Pareto, modified Weibull method,[42–47] bivariate modified Weibull,[48,49] traditional Weibull fit, and Gumbel fit; these are just a few examples of fitting techniques. In the simplest instance, PDFs pX1 and p_{X_2} may represent two identically distributed processes, $X_1(t)$ and $X_2(t)$, with $p_{X_1} = p_{X_2}$.

The alternative (A) scenario, in which processes $X_1(t)$ and $X_2(t)$ have similar distributions, is the subject of this study. Therefore, the objective of the current study would be to locate component PDF p_{X_1} such that it can produce a directly calculated PDF p_X as in instance (A)

$$p_X = \text{conv}\left(p_{X_1}, p_{X_1}\right) \tag{2}$$

restricting our investigation to a single de-convolution illustration to illustrate the later idea of improving a given empirical PDF, p_X, by robustly estimating the unknown PDF, p_{X_1}. Convolution of the two vectors, $\boldsymbol{u}$ and $\boldsymbol{v}$, occurs at the area where the vectors' constituent parts (supports) overlap, with vector $\boldsymbol{v}$ gliding over vector $\boldsymbol{u}$. Convolution is analogous to multiplying two polynomials, whose coefficients are parts of $\boldsymbol{u}$ and $\boldsymbol{v}$, in algebra. Let $\boldsymbol{w}$ be a vector of length $m + n - 1$, with the k-th element being $m + n - 1$, and $\boldsymbol{n}$ be a vector of length$(\boldsymbol{u}, \boldsymbol{v})$, with = length$(\boldsymbol{u})$ and n = length$(\boldsymbol{v})$

$$w(k) = \sum_{j=1}^{m} u(j)v(k - j + 1). \tag{3}$$

All j values that produce acceptable subscripts for $u(j)$ and $v(k - j + 1)$, particularly $j = \max(1, k + 1 - n)$: $1 : \min(k, m)$, are summed. The main scenario in this section is when $m = n$, and one may obtain

$$\begin{gathered} w(1) = u(1) \cdot v(1) \\ w(2) = u(1) \cdot v(2) + u(2) \cdot v(1) \\ w(3) = u(1) \cdot v(3) + u(2) \cdot v(2) + u(3) \cdot v(1) \\ \cdots \\ w(n) = u(1) \cdot v(n) + u(2) \cdot v(n - 1) + \\ \ldots + u(n) \cdot v(1) \\ \cdots \\ w(2n - 1) = u(n) \cdot v(n) \end{gathered} \tag{4}$$

Having established $\boldsymbol{u} = \boldsymbol{v} = (u(1), \ldots, u(n))$, one may now infer from Equation (4) that one obtains increasingly lower amounts of the $\boldsymbol{w}$ - -components $w(n + 1), \ldots, w(2n - 1)$ as the index increases from $n + 1$ to $2n - 1$. The latter, which is twice as long as the original $\boldsymbol{u}$ -distribution support domain and doubles the length of the p_X distribution support, $(2n - 1) \cdot \Delta x \approx 2n \cdot \Delta x = 2X_L$ compared with the original distribution support length $n \cdot \Delta x = X_L$, with Δx being a constant discrete distribution bin width, clearly extends vector w into a wider support domain. The empirical target PDF p_X is discretely represented by the vector $\boldsymbol{w} = (w(1), \ldots, w(n))$, where n is the length of the distribution support, $[0, X_L]$, and this research study is limited to the situation of non-negative valued one-sided random variables, that is, $X \geq 0$, for simplicity.

In this study, only the same distribution scenario—that is, the case when Equation (4) holds equality and $\boldsymbol{u} = \boldsymbol{v}$—will be investigated. Vectors $\boldsymbol{w}$ and $\boldsymbol{u}$ are represented by the PDFs p_X and p_{X_1} in Equation (2), respectively. The unknown components $\boldsymbol{u} = \boldsymbol{v} = (u(1), \ldots, u(n))$ may be estimated progressively, starting with the first component $u(1) = \sqrt{w(1)}$, then the second $u(2) = \frac{w(2)}{2u(1)}$, and so on, until the last one $u(n)$, according to Equation (4), given the values of $\boldsymbol{w} = (w(1), \ldots, w(n))$. In this article, the authors promote a straightforward linear extrapolation of the self-deconvoluted vector $(u(1), \ldots, u(n))$ toward $(u(n + 1), \ldots, u(2n - 1))$; in other words, the PDF tail of p_{X_1} will be linearly extrapolated within the support range $(X_L, 2X_L)$. Given that PDF p_{X_1} is a discrete representation of the associated estimated vector $\boldsymbol{u}$, it is possible to refer to it as a deconvoluted PDF. Using Equation (3), the initial vector $\boldsymbol{w}$ will be doubled in length and projected into the PDF support domain, resulting in a p_X support length$(2n - 1) \cdot \Delta x \approx 2n \cdot \Delta x = 2X_L$ that is twice as long as the original PDF support length $n \cdot \Delta x = X_L$. Since the original (raw) PDF tail, calculated by MC simulations or observations, p_X is typically not smooth, authors suggest smoothening the original PDF $p_X(x)$ tail by interpolation, as cumulative density function (CDF) tail being more regular for higher tail values x. The modified Weibull approach has been used; for $x \geq x_0$, the PDF tail behaves very similarly to $\exp\{-(ax+b)^c + d\}$, where a, b, c, d are appropriate constants fitted for the appropriate x_0, see Equations (6) and (7). Authors have used linear tail extrapolation of p_{X_1} since it is an objective, numerically more stable choice. Biases and assumptions are commonly used in nonlinear extrapolation approaches.

The assumptions of the underlying data's stationarity, ergodicity, quality, and sufficiency are identical to the typical restrictions of any extrapolation approach of this type and apply to the recommended strategy as well. As previously mentioned, the PDF/CDF distribution tail may be extrapolated using the de-convolution extrapolation technique without the need for a specific extrapolation functional or parametric class. Since projecting exceedance probability is crucial in the majority of reliability analysis engineering applications, 1−CDF extrapolation is required rather than marginal PDF. The complementary cumulative density function 1−CDF will thus be denoted in this research using the same notation as the marginal PDF, f_X. A portion of the original data set (called here "shorter" data set) has been extrapolated to validate the extrapolation procedure indicated above, and estimations based on the entire (called here "longer") data set are compared with the extrapolated data. Therefore, the purpose of this work is to demonstrate the effectiveness of the recommended extrapolation technique over at least a few orders of magnitude.

In contrast to the marginal PDF, where one may utilize 1-CDF and then use integration to create a new, smoother CDF, an iterative approach may be used, as the previous manner of explanation demonstrates. To estimate the deconvoluted 1-CDF distribution f_{X_1} given an empirical distribution f_X, described in the preceding section, the discrete convolution approach, or rather deconvolution, has been built on sequentially solving Equation (4). As was previously predicted for the empirical parent PDF/CDF distribution f_X, the resultant deconvoluted vector $\boldsymbol{u} = (u(1), \ldots, u(n))$ components $u(j)$ are often monotonously decreased with increasing index j. Some of the final values of the resulting vector $\boldsymbol{u}$, such as $(u(n-L), \ldots, u(n))$, may go negative for some $L < n$. The pivot value is the lowest positive value f_L of a particular distribution tail of f_X. The scaling is then a linear transformation on a decimal-log scale along the PDF's vertical y-axis

$$g_X = \mu(\log_{10}(f_X) - \log_{10}(f_L)) + \log_{10}(f_L) \quad (5)$$

with the reference level f_L being constant and $g_X(x)$ being a scaled $\log_{10}$ version of the empirical base distribution f_X. To prevent the occurrence of negative components in the resultant f_{X_1}, the scaling coefficient μ may be selected. When $\tilde{f}_X = \mathrm{conv}(f_{X_1}, f_{X_1})$ as in Equation (2) was used to get f_{X_1}, the original scale was restored by performing an inverse scaling μ^{-1} with $\tilde{f}_X$ being the target extrapolated version of f_X.

2.1 | Modified Weibull extrapolation

We now include a comment on the "shorter" data record PDF/CDF distribution tail f_X interpolation problem. The latter interpolation was required since the empirical PDF f_X is frequently an inappropriate input for Equation (4) due to its inherently extremely irregular tail section. Because of this, a straightforward modified Weibull (Naesss–Gaidai) extrapolation form has been used

$$f_X(x) \approx \exp\{-(ax+b)^c + d\}, x \geq x_0 \quad (6)$$

using the appropriate optimisation method, reduce the mean square error function F with respect to the four constant parameters a, b, c, d.

$$\boldsymbol{F}(\boldsymbol{a}, \boldsymbol{b}, \boldsymbol{c}, \boldsymbol{d}) = \int_{\boldsymbol{x_0}}^{\boldsymbol{X_L}} \boldsymbol{h}(\boldsymbol{x})\{\ln(\boldsymbol{f_X}(\boldsymbol{x})) - \boldsymbol{d} + (\boldsymbol{ax}+\boldsymbol{b})^{\boldsymbol{c}}\}^2 \, \boldsymbol{dx}, \boldsymbol{x} \geq \boldsymbol{x_0} \quad (7)$$

with the probability distribution tail $(x > x_0)$ becoming pre-asymptotically regular at the beginning of the extrapolation tail area, where x_0 serves as an appropriate tail marker. There are several methods to construct the weight function h, such as $h(x) = \{\ln C^+(x) - \ln C^-(x)\}^{-2}$ with $(C^-(x), C^+(x))$ is the confidence interval (CI), which is experimentally calculated using simulated or observed data.

When performing modified Weibull multi-parameter fit, such as parametric nonlinear extrapolation, room for error and prediction instability can be significant due to variability in estimated model parameters and extrapolation's nonlinearity. This is one advantage of the proposed methodology over other extrapolation methods.

3 | MODEL IN BRIEF

Without the use of any presumptions, linearizations, or other oversimplifications, the environmental data from the monitored buoys were post-processed into the empirical multidimensional joint probability distribution function (PDF). This study used the power law formula $U(z) = U(z_r)\left(\frac{z}{z_r}\right)^{\alpha}$ to extrapolate wind speed, where $U(z)$ and $U(z_r)$ represent the wind speed at height z and the reference wind speed at height z_r, respectively. Surface roughness length is denoted by z_0, and the power law constant is equal to $\alpha = 0.14$. The in situ metocean data were then used to quickly estimate the joint PDF $p(U, H_s T_p)$, which produced a three-dimensional (3D) dispersed diagram with H_s and T_p standing for significant wave height and peak-spectral period, respectively. This strategy promotes the direct long-term MC simulation method,[40,42–46,48,49] which has the benefit of not relying on any assumptions or simplifications. A semi-submersible FOWT model with one main column and three outer offset columns is shown in Figure 2.

The primary structural dimensions of the semi-submersible FOWT are shown in Table 1. The term "center of mass" (CM).

On top of the DeepCwind platform that was partially submerged, the 5-MW NREL baseline wind turbine was built. To correlate the relevant aerodynamic and gravitational FOWT stresses with its in situ structural dynamics, FAST and AeroDyn were used.[50] The validation of floating offshore wind turbine modeling methods using experimental data had been the subject of substantial experimental work.[2,3,33]

For this work, the aero-hydro-servo-elastic simulation code OpenFAST[25] was used. TurbSim,[27] with generated random wind fields on a 31×31 square grid having 145 m width, using the Kaimal spectral and exponential coherence models. When using the blade element momenta approach and taking into account rotor-wake effects, dynamic stall, and baseline responses, the OpenFAST code module AeroDyn is adequate to describe FOWT aerodynamics. The motion equations of the coupled rigid-flexible system have been solved to determine the structural dynamic responses in the time domain. The Kane technique was used to create these equations of motion, using HydroDyn,[28] incorporating potential flow theory and Morison's equation for large-diameter constructions, to estimate hydrodynamic stresses. Potential flow theory has been used to forecast hydrodynamic coefficients in the frequency domain, such as additional mass and potential damping coefficients. To account for viscous drag forces occurring on FOWT, Morison's formulation incorporated a drag force component. The MoorDyn mooring module, which is based on the lumped mass theory, is used to represent the three catenary mooring lines of the NERL 5 MW semi-submersible FOWT. For extrapolation to predict ultimate loads with a desired return time of 50 years, at least 15

TABLE 1 Semi-submersible floating offshore wind turbine main dimensions.

Item	Value
Platform draft	20.0 m
Spacing between offset columns	50.0 m
Length of base columns	6.0 m
Diameter of main column	6.5 m
Diameter of base columns	24.0 m
Platform mass	$1.347 \cdot 10^{7}$ kg
Platform roll inertia, about CM	$6.827 \cdot 10^{9}$ kg m^2
Platform pitch inertia, about CM	$6.827 \cdot 10^{9}$ kg m^2
Platform yaw inertia, about CM	$1.226\text{E} \cdot 10^{10}$ kg m^2

Abbreviation: CM, center of mass.

FIGURE 2 Left: DeepCwind semi-submersible floating offshore wind turbine (FOWT) platform 1/50 scale model.[30,32] Right: An example of operating FOWT.

quick simulations lasting 10 min are required under typical production circumstances. International Electro-Technical Commission IEC-61400-1. According to the IEC Design Load Case (DLC), a total of 2550 10 min short-term random cases are chosen and numerically simulated in this study, ranging from a cut-in wind speed of 3 m/s to a cut-off wind speed of 25 m/s. The duration of each simulation was set to 800 s, with the first 200 s postprocessing being omitted owing to initial transient effects. Three wind speeds U (7, 11, and 15 m/s) have been chosen as load situations in this study just as examples.

The fore-aft bending moment average value of the tower base is larger than zero as a result of the aerodynamic and hydrodynamic loadings. When subjected to large in situ wind forces, excessive structural loads are more likely to reach a particular, extreme value. Additionally, an apparent fluctuation component has been noted; hence, strong structural stresses are produced by aerodynamic and hydrodynamic forces. Extensive experimental work has been done within the context of the OC3 projects,[26–33] to provide experimental data and test FOWT numerical modeling methodologies. The modeling skills of OpenFAST, the numerical simulation tool chosen for this investigation, have been confirmed by the numerical and experimental results.

4 | RESULTS

This work presents the methodology for computing the FOWT severe bending moment response. The groundbreaking de-convolution method has been described in previous sections. The recommended method efficiently uses all the available information to precisely predict extreme values. Based on the overall effectiveness of the suggested strategy, it was found that the novel de-convolution methodology could include environmental information and provide more accurate forecasts.[36-38,51-56]

Figure 3 shows the final un-scaled results of the proposed de-convolution technique in this paper, namely the "shorter" decimal log scale f_X PDF tail, extrapolated by de-convolution, along with "longer" data distribution tail and modified Weibull Naess–Gaidai (NG) extrapolation. Equidistant sampling was utilized to reduce the size of the "shorter" data collection by 50 times compared to the entire "longer" simulated data set.

Figure 4, similar to Figure 3, presents the final un-scaled results of the proposed de-convolution technique in this paper, namely the "shorter" decimal log scale f_X PDF tail, extrapolated by de-convolution, along with "longer" data distribution tail and modified Weibull (NG) extrapolation. Different wind speeds U have been

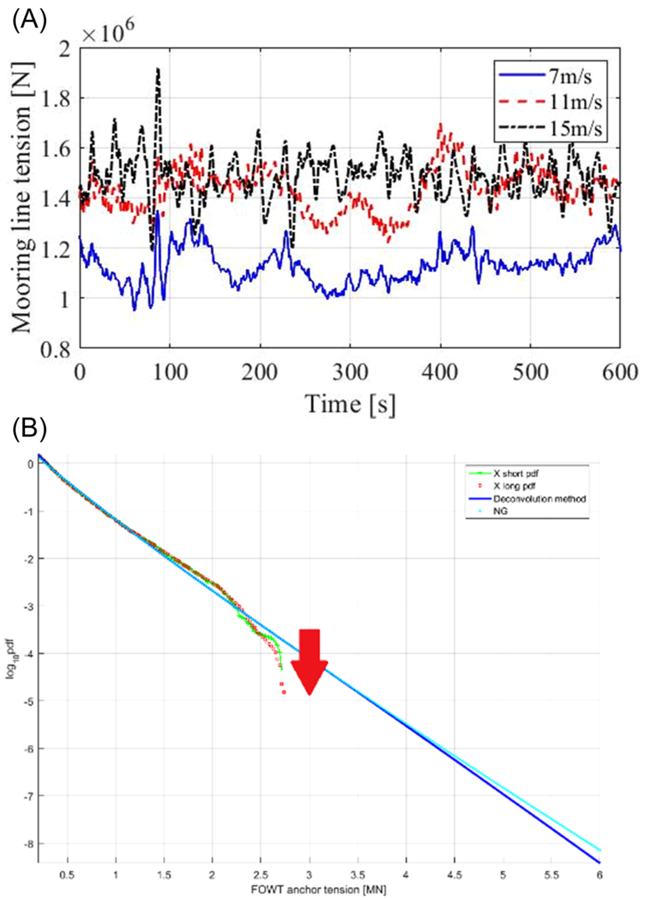

FIGURE 3 (A) Mooring (anchor) tension time series. (B) Response predictions for floating offshore wind turbine anchor tension. Un-scaled "shorter" decimal log scale f_X tail, raw (green) and extrapolated by de-convolution (solid blue line, along with "longer" data (red line) and modified Weibull (cyan line).

combined according in situ wind speed probabilities scatter diagram, following the long-term analysis flowchart Figure 1 right, to obtain realistic extreme response predictions. In Figures 3 and 4, red arrows indicate the directional difference between "shorter" and "longer" data sets, indicating that proposed deconvolution technique yields more accurate results than the modified Weibull fit.

Equidistant sampling was utilized to reduce the size of the "shorter" data collection by 50 times compared to the entire "longer" simulated data set. It should be emphasized that it is hard to come to a firm judgment on the precision of the suggested de-convolution approach using the FOWT response data set; yet, it can be seen from Figures 3 and 4 that the proposed method agrees well with the modified Weibull method, being based on the "shorter" data set, and delivering distribution quite close to the one based on the "longer" data set. It is also seen from Figures 3 and 4 that the proposed de-convolution technique performs slightly better than modified Weibull fit.

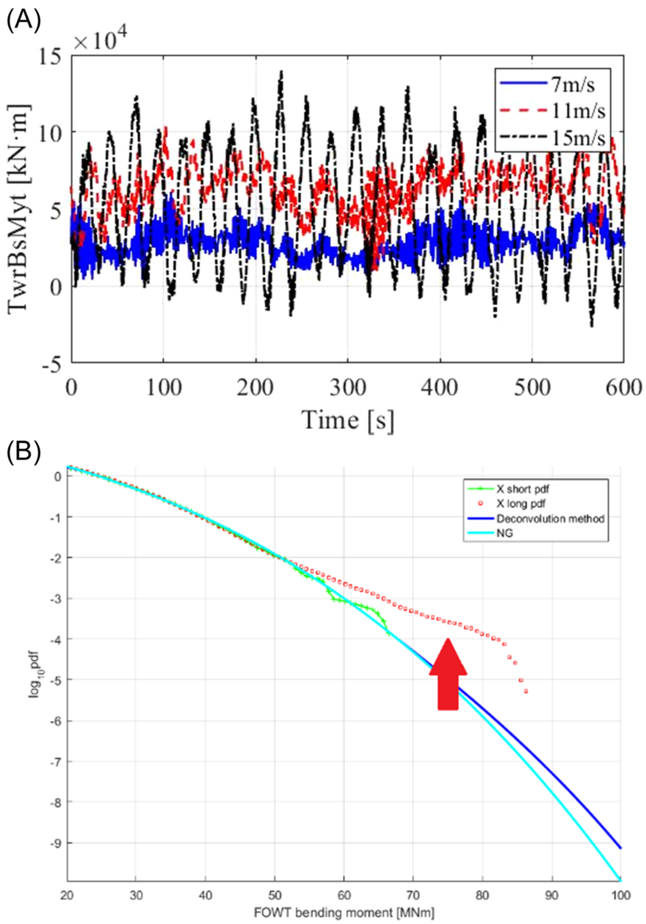

FIGURE 4 (A) Platform tower base fore-aft bending moment (TwrBsMyt) sample time series for various wind speeds $\boldsymbol{U}$. (B) Floating offshore wind turbine tower-base fore-aft bending moment predictions. Un-scaled "shorter" decimal log scale f_X PDF tail, raw (green) and extrapolated by de-convolution (solid blue line), along with "longer" data (red line) and modified Weibull (cyan line).

5 | CONCLUSIONS

It has been suggested to estimate the FOWT characteristic design values using a unique de-convolution technique. This study analyzed FOWT anchor tensions, as well as its structural bending moments, occurring as a result of in situ environmental loads.

The described technique has the following advantages:

- Various datasets, such as those that are numerically simulated or quantitatively measured, may be explored.
- Unlike other techniques like three-parameter Weibull, modified Weibull, Gumbel, and POT, the proposed strategy does not depend on any pre-assumed functional family to perform reliable distribution tail extrapolation.

Additionally, it should be kept in mind that the offered technique may have technical benefits beyond simply anticipating severe FOWT responses. The reason for better performance of the suggested deconvolution technique is that, opposite to the modified Weibull method, the proposed deconvolution method is less reliant on preassumed functional class, highly nonlinear, and potentially unstable in extrapolation.

A major limitation of the advocated approach lies within the system stationarity assumption, which is reasonable within short-term 3 h stationary sea state conditions, often used in offshore engineering, but may not be the case for long-term analysis. Dynamic FOWT systems may become nonstationary in the presence of an underlying trend; for example, system degradation due to corrosion or fatigue damage. If the latter is the case, one should first identify and subtract the underlying trend and only then use the methods advocated in this study. This study advocated a general-purpose reliability approach, being well suitable not only for wave- and wind-induced loads but for any combination of in situ environmental loads.

DATA AVAILABILITY STATEMENT

Data will be available on request. For environmental data, see [23].

ORCID

Oleg Gaidai http://orcid.org/0000-0002-3196-8562

REFERENCES

1. Bayati I, Jonkman J, Robertson A, Platt A. The effects of second-order hydrodynamics on a semi-submersible floating offshore wind turbine. *J Phys Conf Ser*. 2014;524(1):012094.
2. Benitz MA, Schmidt DP, Lackner MA, Stewart GM, Jonkman J, Robertson A. *Validation of Hydrodynamic Load Models Using CFD for the OC4-DeepCwind Semi-Submersible*. National Renewable Energy Lab. (NREL); 2015.
3. Coulling AJ, Goupee AJ, Robertson AN, Jonkman JM, Dagher HJ. Validation of a FAST semi-submersible floating wind turbine numerical model with DeepCwind test data. *J Renewable Sustain Energy*. 2013;5(2):023116.
4. Dimitrov N. Comparative analysis of methods for modelling the short-term probability distribution of extreme wind turbine loads. *Wind Energy*. 2016;19(4):717-737.
5. Ernst B, Seume JR. Investigation of site-specific wind field parameters and their effect on loads of offshore wind turbines. *Energies*. 2012;5(10):3835-3855.
6. Fogle J, Agarwal P, Manuel L. Towards an improved understanding of statistical extrapolation for wind turbine extreme load. *Wind Energy*. 2008;11(6):613-635.
7. International Electrotechnical Commission. *IEC 61400-1: Wind Turbines Part 1: Design Requirements*. International Electrotechnical Commission; 2005:177.

8. Gaidai O, Cao Y, Loginov S. Global cardiovascular diseases death rate prediction. *Curr Probl Cardiol*. 2023;48(5):101622. doi:10.1016/j.cpcardiol.2023.101622
9. Gaidai O, Cheng Y, Xu X, Su Y. Long-term offshore Bohai bay Jacket strength assessment based on satellite wave data. *Ships Offshore Struct*. 2018;13(6):657-665. doi:10.1080/17445302.2018.1444346
10. Gaidai O, Xu J, Yan P, Xing Y, Zhang F, Wu Y. Novel methods for wind speeds prediction across multiple locations. *Sci Rep*. 2022;12:19614. doi:10.1038/s41598-022-24061-4
11. Gaidai O, Wang F, Wu Y, Xing Y, Medina A, Wang J. *Offshore Renewable Energy Site Correlated Wind-Wave Statistics*. Vol 68. Probabilistic Engineering Mechanics; 2022. doi:10.1016/j.probengmech.2022.103207
12. Gaidai O, Xu J, Hu Q, Xing Y, Zhang F. Offshore tethered platform springing response statistics. *Sci Rep*. 2022;12. www.nature.com/articles/s41598-022-25806-x
13. Gaidai O, Xing Y, Xu X. Novel methods for coupled prediction of extreme wind speeds and wave heights. *Sci Rep*. 2023. doi:10.1038/s41598-023-28136-8
14. Moan T, Gao Z, Bachynski EE, Nejad AR. Recent advances in integrated response analysis of floating wind turbines in a reliability perspective. *J Offshore Mech Arctic Eng*. 2020;142(5).
15. Zhang X, Sun L, Sun H, Guo Q, Bai X. Floating offshore wind turbine reliability analysis based on system grading and dynamic FTA. *J Wind Eng Ind Aerodyn*. 2016;154:21-33.
16. Li H, Soares CG, Huang HZ. Reliability analysis of a floating offshore wind turbine using Bayesian networks. *Ocean Eng*. 2020;217:107827.
17. Xu X, Xing Y, Gaidai O, et al. A novel multi-dimensional reliability approach for floating wind turbines under power production conditions. *Front Mar Sci*. 2022;9. doi:10.3389/fmars.2022.970081
18. Song Y, Basu B, Zhang Z, Sørensen JD, Li J, Chen J. Dynamic reliability analysis of a floating offshore wind turbine under wind-wave joint excitations via probability density evolution method. *Renew Energy*. 2021;168:991-1014.
19. Liu H, Zhao C, Ma G, He L, Sun L, Li H. Reliability assessment of a floating offshore wind turbine mooring system based on the TLBO algorithm. *Appl Ocean Res*. 2022;124:103211.
20. Sultania A, Manuel L. Reliability analysis for a spar-supported floating offshore wind turbine. *Wind Eng*. 2018;42(1):51-65.
21. Zhang J, Kang J, Sun L, Bai X. Risk assessment of floating offshore wind turbines based on fuzzy fault tree analysis. *Ocean Eng*. 2021;239:109859.
22. Accessed January, 2023. https://www.ndbc.noaa.gov/station_page.php?station=46041
23. International Electrotechnical Commission. *IEC 61400-3. Wind Turbines Part 3: Design Requirements for Offshore Wind Turbines*. 2009.
24. Jonkman JM, Buhl, ML Jr. New developments for the NWTC's FAST aeroelastic HAWT simulator. ASME Wind Energy Symposium, 42nd AIAA Aerospace Sciences Meeting and Exhibit, Reno Nevada, USA, New York. 2004.
25. Jonkman JM, Buhl, ML Jr. *FAST User's Guide*. National Renewable Energy Laboratory. 2005. Technical Report No. NREL/EL-500-38230.
26. Jonkman JM, Buhl, ML Jr. Loads analysis of a floating offshore wind turbine using fully coupled simulation. Wind-Power 2007 Conference & Exhibition. 2007.
27. Jonkman BJ. *TurbSim User's Guide: Version 1.50 (No. NREL/TP-500-46198)*. National Renewable Energy Lab. (NREL); 2009.
28. Jonkman JM, Robertson A, Hayman GJ. *HydroDyn User's Guide and Theory Manual*. National Renewable Energy Laboratory; 2014.
29. Li L, Hu Z, Wang J, Ma Y. Development and validation of an aero-hydro simulation software for offshore floating wind turbine. *J Ocean Wind Energy*. 2015;2(1):1-11.
30. Li H, Hu Z, Wang J, Meng X. Short-term fatigue analysis for tower base of a spar-type wind turbine under stochastic wind-wave loads. *Int J Nav Archit Ocean Eng*. 2018;10(1):9-20.
31. Liu Y, Yoshida S, Yamamoto H, Toyofuku A, He G, Yang S. Response characteristics of the DeepCwind floating wind turbine moored by a single-point mooring system. *Appl Sci*. 2018;8(11):2306.
32. Robertson A, Jonkman J, Masciola M, et al. *Definition of the Semi-Submersible Floating System for Phase II of OC4* (No. NREL/TP-5000-60601). National Renewable Energy Lab. (NREL); 2014.
33. Robertson AN, Wendt F, Jonkman JM, et al. OC5 project phase II: validation of global loads of the DeepCwind floating semi-submersible wind turbine. *Energy Procedia*. 2017;137:38-57.
34. Gaidai O, Xing Y. A novel multi regional reliability method for COVID-19 death forecast. *Eng Sci*. 2022;21. doi:10.30919/es8d799
35. Gaidai O, Xing Y. A novel bio-system reliability approach for multi-state COVID-19 epidemic forecast. *Eng Sci*. 2022;21. doi:10.30919/es8d797
36. Gaidai O, Yan P, Xing Y. Future world cancer death rate prediction. *Sci Rep*. 2023;13(1). doi:10.1038/s41598-023-27547-x
37. Gaidai O, Wu Y, Yegorov I, Alevras P, Wang J, Yurchenko D. Improving performance of a non-linear absorber applied to a variable length pendulum using surrogate optimisation. *J Vib Control*. 2022. doi:10.1177/10775463221142663
38. Gaidai O, Yan P, Xing Y. Prediction of extreme cargo ship panel stresses by using deconvolution. *Front Mech Eng*. 2022;8. doi:10.3389/fmech.2022.992177
39. Xu X, Gaidai O, Naess A, Sahoo P. Extreme loads analysis of a site-specific semi-submersible type wind turbine. *Ships Offshore Struct*. 2020;15(suppl 1):S46-S54.
40. Gaidai O, Cao Y, Xing Y, Wang J. Piezoelectric energy harvester response statistics. *Micromachines*. 2023;14(2):271. doi:10.3390/mi14020271
41. Gaidai O, Xing Y, Xu X. *COVID-19 Epidemic Forecast in USA East Coast by Novel Reliability Approach*. Research Square; 2022. doi:10.21203/rs.3.rs-1573862/v1
42. Xu X, Xing Y, Gaidai O, et al. A novel multi-dimensional reliability approach for floating wind turbines under power production conditions. *Front Marine Sci*. 2022;9. doi:10.3389/fmars.2022.970081
43. Gaidai O, Xing Y, Balakrishna R. Improving extreme response prediction of a subsea shuttle tanker hovering in ocean current using an alternative highly correlated response signal. *Result Eng*. 2022;15. doi:10.1016/j.rineng.2022.100593
44. Cheng Y, Gaidai O, Yurchenko D, Xu X, Gao S. Study on the dynamics of a payload influence in the polar ship. The 32nd International Ocean and Polar Engineering Conference, Paper Number: ISOPE-I-22-342; 2022.

45. Balakrishna R, Gaidai O, Wang F, Xing Y, Wang S. A novel design approach for estimation of extreme load responses of a 10-MW floating semi-submersible type wind turbine. *Ocean Eng*. 2022;261. doi:10.1016/j.oceaneng.2022.112007
46. Gaidai O, Yan P, Xing Y, Xu J, Wu Y. A novel statistical method for long-term coronavirus modelling. F1000 Research. 2022. Accessed January 1, 2023. https://orcid.org/0000-0003-0883-48542
47. Zhang J, Gaidai O, Gao J. Bivariate extreme value statistics of offshore jacket support stresses in Bohai bay. *J Offshore Mech Arctic Eng*. 2018;140(4):041305. doi:10.1115/1.4039564
48. Gaidai O, Wang K, Wang F, Xing Y, Yan P. Cargo ship aft panel stresses prediction by de-convolution. *Marine Structures*. 2022;88. doi:10.1016/j.marstruc.2022.103359
49. Gaidai O, Xu J, Xing Y, et al. Cargo vessel coupled deck panel stresses reliability study. *Ocean Eng*. 2022;268. doi:10.1016/j.oceaneng.2022.113318
50. Jonkman J, Buhl M. *FAST User's Guide*. NREL; 2005. NREL/EL-500-38230.
51. Næss A, Gaidai O, Teigen P. Extreme response prediction for non-linear floating offshore structures by Monte Carlo simulation. *Appl Ocean Res*. 2007;29(4):221-230.
52. Stewart GM, Robertson A, Jonkman J, Lackner MA. The creation of a comprehensive metocean data set for offshore wind turbine simulations. *Wind Energy*. 2016;19: 1151-1159.
53. Gaidai O, Wang F, Xing Y, Balakrishna R. Novel reliability method validation for floating wind turbines. Advanced Energy and Sustainability Research. 2023. doi:10.1002/aesr.202200177
54. Jain A, Robertson AN, Jonkman JM, Goupee AJ, Kimball RW, Swift AHP. *FAST Software Verification of Scaling Laws for DeepCwind Floating Wind System Tests*. 2012. NREL Report No. CP-5000-54221.
55. Gaidai O, Xing Y. Novel reliability method validation for offshore structural dynamic response. *Ocean Eng*, 266(5). doi:10.1016/j.oceaneng.2022.113016
56. Jian Z, Gaidai O, Gao J. Bivariate extreme value statistics of offshore jacket support stresses in Bohai bay. *J Offshore Mech Arctic Eng*. 2018;140(4).

How to cite this article: Liu Z, Gaidai O, Sun J, Xing Y. Deconvolution approach for floating wind turbines. *Energy Sci Eng*. 2023;11:2742-2750. doi:10.1002/ese3.1485